

A Consideration of Human-Unicycle Model for Unicycle Operation Analysis based on Moment Balancing Point

Hiroshi OHSAKI

Department of Computers and System Engineering
Tokyo Denki University
2-2 Kanda-Nishiki-cho, Chiyoda-ku, Tokyo, Japan
ohsaki@hatalab.k.dendai.ac.jp

Masami IWASE, Teruyoshi SADAHIRO, Shoshiro HATAKEYAMA

Department of Robotics and Mechatronics
Tokyo Denki University
Tokyo, Japan
{iwase, sadahiro, sho}@fr.dendai.ac.jp

Abstract—The unicycle operation is a good exercise for training of the sense of balance, the agility and the ability to coordinate the body according to situations. This paper aims to give an interpretation of the relationship between the moment balancing point (MBP) and the center of pressure (CP) in a riding a unicycle from the human motion viewpoint. This paper shows derivations of Human-Unicycle model motion equations according to the Projection Method, and represents the relationship between the MBP and the CP of the the model by considering structure and constraint reaction forces of the model.

Index Terms—Human-Unicycle model, Projection Method, Modeling, Unicycle operation

I. INTRODUCTION

Riding a unicycle is a good exercise for training of the sense of balance and the coordinate ability to move the body dexterously according to a situation. Elementary schools in Japan have introduced unicycles as standard teaching materials for physical education in the 3rd and 4th grades to train those abilities. A unicycle has relatively higher order and complicated dynamics, and then a sophisticated and skillful feedback from the senses to the whole body motion is required to operate a unicycle. Consequently it probably takes much time for beginners to achieve the feedback. The report of Japan Unicycling Association referred to average practice periods for a variety of trainees. In the report, if a person takes one hour for practice everyday, children in elementary school take a few days averagely, adult persons a week, older persons over 60 years old have more than a month to get a basic unicycle riding skill. Moreover, a unicycle is an unstable vehicle, and the instability hinders beginners from continuous training. Therefore, we have been interested in the analysis of the progress with the skill of riding unicycle, and have aimed to develop an assistive system for every rider to achieve the unicycle riding skill.

A practical training simulator of a unicycle is very useful to provide the exercise environment for trainees, and also to provide the experimental system for us to analyze and feedback the rider's information, and to realize any assistive system. We have developed a practical training unicycle simulator consisting of a 6-degree-of-freedom Stewart platform, a virtual

visualizing system, a measurement system and a control system to integrate those of systems [1]. The workflow of this simulator is as follows: 1) the informations from the measurement system are transmitted to the control system, 2) the behavior of a virtual unicycle is simulated according to the informations, 3) the motion of the behavior is carried out by the Stewart platform, and 4) the visual information corresponding to the behavior is also realized by the virtual visualizing system. Thus this simulator can realize both realistic and virtual behavior of unicycles changing the virtual unicycle dynamics in the control system.

A planar unicycle model has been utilized to analyze and evaluate the skill of riding unicycle as the first step because the full model was complicated to use it for getting some initial guess and an expert pointed out that the instability in the sagittal plane is dominant in the unicycle case. We have proposed an evaluation method of the unicycle operation skill with the moment balancing point and the center of pressure on the saddle surface. The moment balancing point on the saddle surface has been defined as a point on the saddle surface to which any force should be applied for cancelling the rotational moment around the saddle pivot. A moment balancing point and a center of pressure abbreviated to MBP and CP, respectively. It has been found that skill of riding unicycle can be classified into skillful and beginners operations according to the relationship between the MBP and the CP. Using the classification as an evaluation, we finally observed that a simple PD feedback control to stabilize the saddle angle weakly was effective to support the beginners training of unicycle riding using our unicycle simulator [2].

This paper aims to give an interpretation of the relationship between the MBP and the CP from the human motion viewpoint. If we aim to develop an assistive system using the evaluation method based on the MBP and the CP, how to feedback the current information of the MBP and the CP to the rider is important to improve his riding skill. Thus, the relationship among the MBP, the CP, and the body motion is required to realize such an assistive system. Human-Unicycle models seem useful for this kind of analysis. Several studies on human-

unicycle models can be found for example in [3]–[7]. Yamafuji et al. [5], [6] reported how to realize a human riding a unicycle by a robot. They developed a robot mimicking a human riding a unicycle, gave the whole structure and model, and proposed a postural stabilizing control with experimental results. These studies are interested as the point that they implied what kind of robot structure is necessary to mimic the human motion. Zenkov and Bloch [7] have also proposed a stabilization of the unicycle with a rider. They introduced a double pendulum model with a wheel regarding the rider as a pendulum, and provided a nonlinear stabilizing controller based on the energy-momentum method for nonholonomic-systems. As mentioned above, several models have been proposed, however, we focus on especially the relationship between the MBP, the CP and the human motion, and then another type of model is necessary to match our demand.

We pay much attention to the posture of the waist and hip because the posture can affect the center of pressure on the saddle surface directly, and then introduce a simple human-unicycle model in which the shape of the rider's waist to hip is taken into account. We say this model as Iwase-Åström model in this paper after the proposer [13]. Iwase-Åström model represents a rider with the link structure. The actions from actuators and the corresponding reactions in the link structure are important in our analysis. Thus the Projection Method [8]–[12] is utilized in this paper to derive those action and reaction relationship as geometric constraints, and also to derive the motion equations of the whole Iwase-Åström model. The Projection Method easily provides those constraints and equations of complicated systems paying attention to the position and/or velocity relationships of all components in the systems. This paper shows those derivations according to the Projection Method, and represents the MBP and the CP of the Iwase-Åström model obviously. Some numerical simulations are performed to check behavior of both the MBP and the CP, and to validate the Iwase-Åström model. We also discuss on the interpretation of the relationship among the MBP, the CP and the body motion from the simulation results.

II. BEHAVIOR OF CP AND MBP IN A UNICYCLE RIDING

One of the difference between beginners and skillful riders of unicycle are behaviors of the saddle on the one hand fall down on the other stabilize near upward direction.

To analyze the behavior, motion equations of a two dimensional unicycle are considered. The unicycle model is shown in Fig. 1. An output result of Body Pressure Measurement System (BPMS) on the seat of the unicycle is shown in Fig. 2. A coordinate system O_{Sheet} is a coordinate axis on the anteroposterior direction in BPMS. The coordinate axis is a line from a point of the saddle to pole position on the saddle. θ_{vs} and θ_{vw} are defined as a wheel angle and a saddle angle of the unicycle. A motion equation of the saddle are obtained as follows:

$$\gamma \cos \theta_{vs} \ddot{\theta}_{vw} + \beta \dot{\theta}_{vs}^2 - \delta \sin \theta_{vs} = u_s, \quad (1)$$

$$\beta = J_s + m_s r_s^2, \quad \gamma = m_s r_s r_w, \quad \delta = g m_s r_s, \quad (2)$$

where u_s is a torque which are generated on the saddle. Here u_s satisfies as follows:

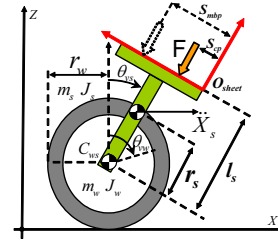


Fig. 1. A two dimensional unicycle model.

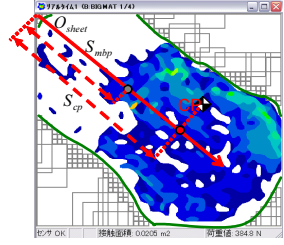


Fig. 2. An output result example of BPMS; A maker shows CP.

TABLE I
PARAMETERS OF THE TWO DIMENSIONAL UNICYCLE MODEL.

saddle mass center moment of inertia	J_s	0.0519 [kgm ²]
saddle mass	m_s	1.643 [kg]
distance between the wheel rotation axis and CoG of the saddle	r_s	0.40 [m]
wheel radius	r_w	0.225 [m]
viscous friction coefficient between wheel and saddle	C_w	0.0677 [Nm · s/rad]
gravity acceleration	g	9.81 [m/s ²]

$$u_s = F(S_{mbp} - S_{cp}), \quad (3)$$

where S_{cp} is a length in which CP is projected in O_{Sheet} , F is a force at a point of S_{cp} .

When the values of S_{mbp} and S_{cp} are equal, the torque is canceled. When a difference between S_{mbp} and S_{cp} is large, the torque become larger shown in Fig. 4. Since the skillful riders librate the saddle angle, the values S_{mbp} and S_{cp} are intersected when the riders is balancing the saddle. Therefore we consider that a difference between beginners and skillful riders appears clearly by comparing S_{mbp} with S_{cp} .

It is necessary to derive S_{mbp} from (3) using measurement torque u_s . Therefore u_s is estimated from (1). Then $\ddot{\theta}_{vw}$ is measured by a gyro sensor attached to the saddle. $\dot{\theta}_{vs}$ and θ_{vs} are obtained by differentiating and integrating with the measured value of the gyro sensor. It is difficult to install the gyro sensor in the wheel, θ_{vw} is derived from a geometrical relation of the unicycle. X_s is a center of gravity coordinate in a direction of X of the saddle, θ_{vw} is derived from the geometrical relation as follows:

$$\ddot{\theta}_{vw} = \frac{\ddot{X}_s + r_s \sin \theta_{vs} \dot{\theta}_{vs}^2 - r_s \cos \theta_{vs} \ddot{\theta}_{vs}}{r_w}. \quad (4)$$

u_s is assumed by substituting these results to (1). And S_{mbp} is obtained from (3).

S_{cp} and S_{mbp} are measured and compared with beginners and skillful riders using an experimental unicycle that is shown in Fig. 3. The BPMS, the gyro sensor and the acceleration sensor are installed in the experimental unicycle. The physical parameters used to derive S_{mbp} are shown in TABLE I. The experimental course is straight that length is 5[m]. Fig. 5 show that CP and MBP crosses frequently in the case of a skillful rider. Fig. 6 show that CP and MBP does not in the case of a beginner.

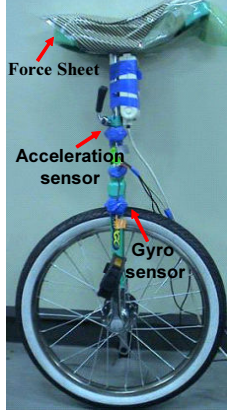


Fig. 3. The experimental unicycle.

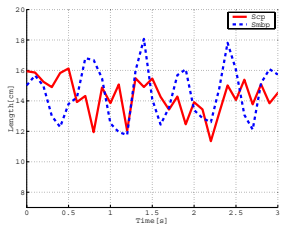


Fig. 5. Behavior of MBP and CP of skillful rider.

Fig. 4. The relationship between CP and MBP: CP is changed a rider's touching point at the saddle. MBP is chaged states of the unicycle and the rider, e.g. the wheel torque.

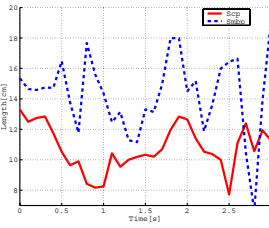


Fig. 6. Behavior of MBP and CP of beginner.

III. MODELING OF A HUMAN-UNICYCLE MODEL

Analyzing the skill acquiring process to ride the unicycle, motion equations of the human-unicycle model is derived (Fig. 8).

Iwase-Åström model has three actuators, which are fixed the body, right thigh and left thigh. Torques which generate from the actuators are inputted indirectly to the saddle and the wheel of Iwase-Åström model. It is easy to consider equilibrium of force of a simple system. However it is difficult to consider equilibrium of force of a complex system which consists a lot of rigid bodies and/or has nonholonomic constraint.

Wherein the Projection Method can derive motion equations and constraint reaction forces of the complex system by describing relations for each rigid body positions and velocities.

A. Outline of the projection method

The outline of the procedure which carries out a modeling of a system using the Projection Method is shown below.

- 1) Define a coordinate systems.
- 2) Define a generalized coordinate \boldsymbol{x} and a generalized velocity \boldsymbol{v} of a unconstrained system.
- 3) Derive motion equations of the unconstrained system.
- 4) Define a generalized mass matrix \boldsymbol{M} and a generalized force \boldsymbol{h} from the motion equations.

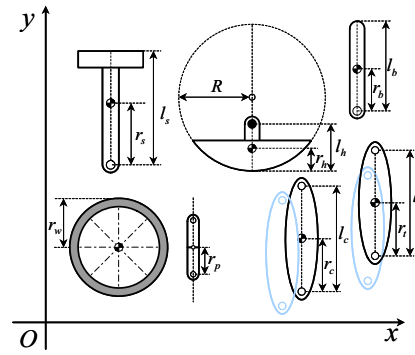
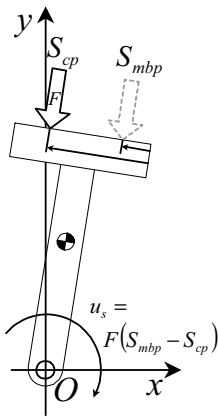


Fig. 7. A unconstrained system of Iwase-Åström model.

- 5) Derive a constraint matrix \boldsymbol{C} which satisfies $\boldsymbol{C}\boldsymbol{v} = \mathbf{0}$ by describing relations for each rigid body positions and velocities of elements of the system.
- 6) Decompose \boldsymbol{v} to the tangent speeds $\dot{\boldsymbol{q}}$ and the other velocity components.
- 7) Derive an orthogonal complement matrix to \boldsymbol{C} which satisfies $\boldsymbol{CD} = \mathbf{0}$ and $\boldsymbol{v} = \boldsymbol{D}\dot{\boldsymbol{q}}$.
- 8) Derive motion equations of the constrained system that is projected motion equations with constraint reaction forces to the tangent space by \boldsymbol{D}^T .

Note that motion equations are derived from the constraint matrix.

B. Generalized coordinate and velocity

An unconstrained system of Iwase-Åström is shown in Fig. 7. A generalized coordinate \boldsymbol{x} and a generalized velocity \boldsymbol{v} are defined in the unconstrained system.

$$\begin{aligned} \boldsymbol{x} &= [\theta_w \ \theta_s \ \theta_h \ \theta_b \\ &\quad x_w \ y_w \ x_s \ y_s \ x_h \ y_h \ x_b \ y_b \\ &\quad x_{tL} \ y_{tL} \ \theta_{tL} \ x_{cL} \ y_{cL} \ \theta_{cL} \ x_{pL} \ y_{pL} \ \theta_{pL} \\ &\quad x_{tR} \ y_{tR} \ \theta_{tR} \ x_{cR} \ y_{cR} \ \theta_{cR} \ x_{pR} \ y_{pR} \ \theta_{pR}]^T, \\ \boldsymbol{v} &= \dot{\boldsymbol{x}}, \end{aligned}$$

where m_{sub} and I_{sub} are the rigid bodies masses and moments of inertia about their mass centers, respectively. θ_{sub} are rotation angles and clockwise directions are positive. ${}_{\text{sub}}$ is subscript which distinguishes each rigid body and meanings are shown in TABLE II.

Motion equations of the unconstrained system is described as follows:

$$m_{\text{sub}}\ddot{x}_{\text{sub}} = F_{x_{\text{sub}}}, \quad (5)$$

$$m_{\text{sub}}\ddot{y}_{\text{sub}} = F_{y_{\text{sub}}}, \quad (6)$$

$$J_{\text{sub}}\ddot{\theta}_{\text{sub}} = \tau_{\text{sub}}. \quad (7)$$

Generalized forces of the unconstrained system are $-m_{\text{sub}}g[\text{N}]$ at the mass centers by gravity acceleration, actuator torques $\tau_b[\text{Nm}]$, $\tau_{tL}[\text{Nm}]$, $\tau_{tR}[\text{Nm}]$ and viscous friction $C_{ws}(\dot{\theta}_w - \dot{\theta}_w)[\text{Nm}]$ at a wheel-saddle joint. The motion

TABLE II
MEANING OF THE SUBSCRIPTS.

wheel	w
saddle	s
hip	h
body	b
left thigh	tL
left cnemis	cL
left pedal	pL
right thigh	tR
right cnemis	cR
right pedal	pR

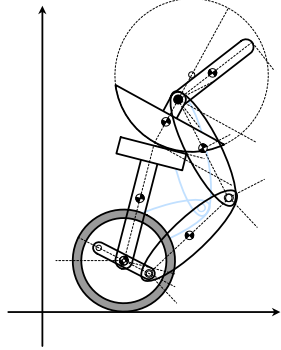


Fig. 8. The proposed new human-unicycle model that is called Iwase-Åström model. The model consists of an upper body as a link, an arc-shape hip, two legs. a saddle, pedals and wheel.

equations of the unconstrained system is

$$M\ddot{x} = h, \quad (8)$$

where

$$\begin{aligned} M &= \text{diag}(J_w, J_s, J_h, J_b, \\ &m_w, m_w, m_s, m_s, m_h, m_h, m_b, m_b \\ &m_{tL}, m_{tL}, J_{tL}, m_{cL}, m_{cL}, J_{cL}, m_{pL}, m_{pL}, J_{pL} \\ &m_{tR}, m_{tR}, J_{tR}, m_{cR}, m_{cR}, J_{cR}, m_{pR}, m_{pR}, J_{pR}), \end{aligned}$$

$$\begin{aligned} h &= [-C_{ws}(\dot{\theta}_w - \dot{\theta}_s) \quad C_{ws}(\dot{\theta}_w - \dot{\theta}_s) \quad -\tau_b - \tau_{tL} - \tau_{tR} \quad \tau_b \\ &0 \quad -m_w g \quad 0 \quad -m_s g \quad 0 \quad -m_h g \quad 0 \quad -m_b g \\ &0 \quad -m_{tL} g \quad \tau_{tL} \quad 0 \quad -m_{cL} g \quad 0 \quad 0 \quad -m_{pL} g \quad 0 \\ &0 \quad -m_{tR} g \quad \tau_{tR} \quad 0 \quad -m_{cR} g \quad 0 \quad 0 \quad -m_{pR} g \quad 0]^T. \end{aligned}$$

C. Constraint equations of the Iwase-Åström model

The Iwase-Åström model consists of an upper body as a link, an arc-shape hip, two legs. a saddle, pedals and a wheel (Fig. 7). The Iwase-Åström model have the positional relation shown in Fig. 8. Position vector of each rigid body is defined as $\mathbf{x}_{\text{sub}} = [x_{\text{sub}} \quad y_{\text{sub}}]^T$. In this coordinate system, the rotation angles are positive to clockwise directions. Therefore rotation matrix $\mathbf{R}(\theta_{\text{sub}})$ defined as follows:

$$\mathbf{R}(\theta_{\text{sub}}) = \begin{bmatrix} \cos \theta_{\text{sub}} & \sin \theta_{\text{sub}} \\ -\sin \theta_{\text{sub}} & \cos \theta_{\text{sub}} \end{bmatrix}.$$

To derive motion equations of the Iwase-Åström, constraint equations are described as below. A positional constraint equation on the wheel which rolls without sliding on the ground is

$$\mathbf{x}_w = \begin{bmatrix} r_w \theta_w \\ r_w \end{bmatrix}. \quad (9)$$

A positional constraint equation on the wheel and the saddle is

$$\mathbf{x}_s = \mathbf{x}_w + \mathbf{R}(\theta_s) \begin{bmatrix} 0 \\ r_s \end{bmatrix}. \quad (10)$$

A positional constraint equation on the saddle and the hip is

$$\begin{aligned} \mathbf{x}_{h_{\text{local}}} &= \mathbf{R}(\theta_h - \theta_s) \begin{bmatrix} 0 \\ -(R - r_h) \end{bmatrix} + \begin{bmatrix} R(\theta_h - \theta_s) \\ R \end{bmatrix}, \\ \mathbf{x}_h &= \mathbf{x}_w + \mathbf{R}(\theta_s) \left(\begin{bmatrix} 0 \\ l_s \end{bmatrix} + \mathbf{x}_{h_{\text{local}}} \right). \end{aligned} \quad (11)$$

A positional constraint equation on the hip and the body is

$$\begin{aligned} \mathbf{x}_{h_{\text{joint}}} &= \mathbf{R}(\theta_h - \theta_s) \begin{bmatrix} 0 \\ -(R - l_h) \end{bmatrix} + \begin{bmatrix} R(\theta_h - \theta_s) \\ R \end{bmatrix}, \\ \mathbf{x}_b &= \mathbf{x}_w + \mathbf{R}(\theta_s) \left(\begin{bmatrix} 0 \\ l_s \end{bmatrix} + \mathbf{x}_{h_{\text{joint}}} \right) + \mathbf{R}(\theta_b) \begin{bmatrix} 0 \\ r_b \end{bmatrix}. \end{aligned} \quad (12)$$

Positional constraint equations on the wheel and pedals are

$$\mathbf{x}_{pL} = \mathbf{x}_w + \mathbf{R}(\theta_w) \begin{bmatrix} 0 \\ r_p \end{bmatrix}, \quad (13)$$

$$\mathbf{x}_{pR} = \mathbf{x}_w + \mathbf{R}(\theta_w) \begin{bmatrix} 0 \\ -r_p \end{bmatrix}. \quad (14)$$

Positional constraint equations on pedals and each cnemides are

$$\mathbf{x}_{cL} = \mathbf{x}_{pL} + \mathbf{R}(\theta_{cL}) \begin{bmatrix} 0 \\ r_c \end{bmatrix}, \quad (15)$$

$$\theta_{pL} = \theta_{cL}, \quad (16)$$

$$\mathbf{x}_{cR} = \mathbf{x}_{pR} + \mathbf{R}(\theta_{cR}) \begin{bmatrix} 0 \\ r_c \end{bmatrix}, \quad (17)$$

$$\theta_{pR} = \theta_{cR}. \quad (18)$$

Positional constraint equations on each cnemis and thigh are

$$\mathbf{x}_{tL} = \mathbf{x}_{pL} + \mathbf{R}(\theta_{cL}) \begin{bmatrix} 0 \\ l_c \end{bmatrix} + \mathbf{R}(\theta_{tL}) \begin{bmatrix} 0 \\ r_t \end{bmatrix}, \quad (19)$$

$$\mathbf{x}_{tR} = \mathbf{x}_{pR} + \mathbf{R}(\theta_{cR}) \begin{bmatrix} 0 \\ l_c \end{bmatrix} + \mathbf{R}(\theta_{tR}) \begin{bmatrix} 0 \\ r_t \end{bmatrix}. \quad (20)$$

Positional constraint equations on joint the hip and each thighs are

$$\begin{aligned} \mathbf{x}_w + \mathbf{R}(\theta_s) \left(\begin{bmatrix} 0 \\ l_s \end{bmatrix} + \mathbf{x}_{h_{\text{joint}}} \right) \\ = \mathbf{x}_{pL} + \mathbf{R}(\theta_{cL}) \begin{bmatrix} 0 \\ l_c \end{bmatrix} + \mathbf{R}(\theta_{tL}) \begin{bmatrix} 0 \\ l_t \end{bmatrix}, \end{aligned} \quad (21)$$

$$\begin{aligned} \mathbf{x}_w + \mathbf{R}(\theta_s) \left(\begin{bmatrix} 0 \\ l_s \end{bmatrix} + \mathbf{x}_{h_{\text{joint}}} \right) \\ = \mathbf{x}_{pR} + \mathbf{R}(\theta_{cR}) \begin{bmatrix} 0 \\ l_c \end{bmatrix} + \mathbf{R}(\theta_{tR}) \begin{bmatrix} 0 \\ l_t \end{bmatrix}. \end{aligned} \quad (22)$$

D. DERIVATION OF A CONSTRAINT MATRIX

The equations (9) to (22) are transformed with following form $\Phi = \mathbf{0}$. Φ is described a 26-dimensional column vector. Then a constraint matrix C which satisfies $Cv = \mathbf{0}$ is derived at

$$C = \frac{\partial \Phi}{\partial x}.$$

E. Derivation of an orthogonal complement matrix to the constraint matrix

The generalized velocity v is decomposed to tangent speeds $\dot{q} = [\dot{\theta}_w \dot{\theta}_s \dot{\theta}_h \dot{\theta}_b]^T$ and the other velocity components that is gathered as v_2 . The tangent speeds consists of angular speeds of the wheel, the saddle, the hip and the body, and v_2 depends on the tangent speeds.

The constraint matrix C decompose to $C = [C_1 \ C_2]$ which satisfies

$$Cv = \mathbf{0}, \quad (23)$$

$$[C_1 \ C_2] \begin{bmatrix} \dot{q} \\ v_2 \end{bmatrix} = \mathbf{0}. \quad (24)$$

An orthogonal complement matrix D satisfies $CD = \mathbf{0}$ and $v = D\dot{q}$ as follows:

$$D = \begin{bmatrix} \mathbf{I} \\ -C_2^{-1}C_1 \end{bmatrix} \quad (25)$$

where \mathbf{I} is identity matrix.

F. Derivation of motion equations

Motion equations with a constraint reaction forces of the system as follows:

$$M\dot{v} = h + C^T \lambda \quad (26)$$

Motion equations of the Iwase-Åström model are obtained by (26) from $v = D\dot{q}$ and $CD = \mathbf{0}$

$$D^T M D \ddot{q} = D^T h - D^T M \dot{D} \dot{q}. \quad (27)$$

IV. MBP AND CP OF THE IWASE-ÅSTRÖM MODEL

A. MBP of the Iwase-Åström model

From the motion equations (27), a motion equation of the saddle is obtained

$$\begin{aligned} M_{IA}(2,1)\ddot{\theta}_w + M_{IA}(2,2)\ddot{\theta}_s + M_{IA}(2,3)\ddot{\theta}_h + M_{IA}(2,4)\ddot{\theta}_b \\ = Dh_{u22}\tau_{tL} + Dh_{u23}\tau_{tR} + D^T(2,:)\mathbf{h}_g \\ + D^T(2,:)\mathbf{h}_q + D^T(2,:)\mathbf{M}\dot{D}\dot{q}, \end{aligned} \quad (28)$$

where a coefficient matrix of \ddot{q} is $D^T M_{IA}$. From (28), the saddle moment of force is $M_{IA}(2,2)\ddot{\theta}_s = \tau_s$.

$$\begin{aligned} \tau_s &= -M_{IA}(2,1)\ddot{\theta}_w - M_{IA}(2,3)\ddot{\theta}_h - M_{IA}(2,4)\ddot{\theta}_b \\ &+ Dh_{u22}\tau_{tL} + Dh_{u23}\tau_{tR} + D^T(2,:)\mathbf{h}_g \\ &+ D^T(2,:)\mathbf{h}_q + D^T(2,:)\mathbf{M}\dot{D}\dot{q}. \end{aligned} \quad (29)$$

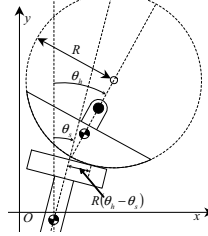


Fig. 9. Center of pressure (CP) of the Iwase-Åström mode

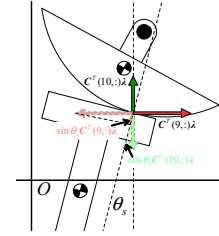


Fig. 10. F is a force at point of CP of the Iwase-Åström mode

TABLE III
DRIVING SIMULATION PARAMETERS OF THE IWASE-ÅSTRÖM MODEL.

r_w	0.281 [m]
r_p	0.125 [m]
r_s	0.453 [m]
l_s	0.562 [m]
r_h	0.050 [m]
l_h	0.060 [m]
R	0.400 [m]
r_b	0.200 [m]
r_t	0.250 [m]
l_t	0.500 [m]
r_c	0.250 [m]
l_c	0.500 [m]
m_w	1.821 [kg]
J_w	0.181 ($\text{kg} \cdot \text{m}^2$)
m_s	1.078 [kg]
J_s	0.148 ($\text{kg} \cdot \text{m}^2$)
m_h	3.500 [kg]
J_h	$10 \frac{m_h r_h^2}{4} [\text{kg} \cdot \text{m}^2]$
m_b	$30.000 [\text{kg}]$
J_b	$10 \frac{m_b r_b^2}{4} [\text{kg} \cdot \text{m}^2]$
m_t	$7.000 [\text{kg}]$
J_t	$\frac{m_t r_t^2}{4} [\text{kg} \cdot \text{m}^2]$
m_c	$3.000 [\text{kg}]$
J_c	$\frac{m_c r_c^2}{4} [\text{kg} \cdot \text{m}^2]$
m_p	$0.200 [\text{kg}]$
J_p	$\frac{m_p r_p^2}{4} [\text{kg} \cdot \text{m}^2]$

1) CP of the Iwase-Åström model: CP is obtained by considering a arc-shape hip of the Iwase-Åström model as follows:

$$CP = R(\theta_h - \theta_s). \quad (30)$$

2) F of the Iwase-Åström model: F which is a force at point of the CP is derived by considering constraint reaction forces of Iwase-Åström model. The constraint reaction forces $C^T \lambda$ is derived from the motion equations (26) as follows:

$$C^T \lambda = C^T (CM^{-1}C^T)^{-1} C (\dot{D}\dot{q} - M^{-1}h). \quad (31)$$

Using part of the constraint reaction forces, the force F is

$$F = \sin \theta_s C^T(9,:)\lambda + \cos \theta_s C^T(10,:)\lambda. \quad (32)$$

From the equations (29), (30) and (32), MBP of the Iwase-Åström model is derived.

V. BEHAVIOR OF MBP AND CP IN DRIVING SIMULATION OF THE IWASE-ÅSTRÖM MODEL

To check behaviors of MBP and CP, driving simulation of the Iwase-Åström model is achieved. Parameters in driving simulation of the Iwase-Åström model are shown in TABLE III. The initial angles of the wheel, the saddle, the hip and the body are 0, and angular velocity of the wheel is

$\dot{\theta}_w = 10\pi[\text{rad/sec}]$. To drive the model stably a control system is designed. It is difficult to design a control system based on nonlinear control theory, because Iwase-Åström model is a complex nonlinear model.

To make control inputs, wherein Iwase-Åström model is divided into the unicycle and the body. Additionally, for simplicity, the divided systems are linearized on upright position. Input torques of Iwase-Åström model are obtained state feedback controls for the divided linearized systems.

The actuator torques τ_{tL}, τ_{tR} are determined by the divided linearized system. A weighting matrix is set to $\mathbf{Q}_{ws} = \text{diag}(10^{-5}, 10^4, 10^{-11}, 1)$ for x_{ws} . A weighting matrix is set to $\mathbf{R}_{ws} = 1$ for u_{ws} . The obtained input u_{ws} from the state feedback is directly inputted to τ_{tL}, τ_{tR} . The body torque τ_b is determined in the same way. A weighting matrix is set to $\mathbf{Q}_b = \text{diag}(1, 10^4)$ for the rotation angle and velocity of the body. A weighting matrix is set to $\mathbf{R}_b = 1$ for τ_b .

In actual unicycle riding, foot of the rider are not fixed to the pedal. Therefore the pedal effort forces are always positive. In this simulation, the torques are derived by considering the fact. Results of the simulation are shown in Fig. 11, Fig. 12, Fig. 13, Fig. 14, Fig. 15 and Fig. 16.

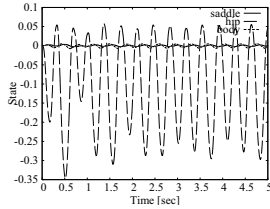


Fig. 11. Angles on the simulation with stabilizing inputs.

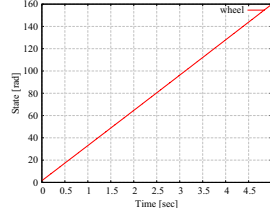


Fig. 12. Wheel angle on the simulation with stabilizing inputs.

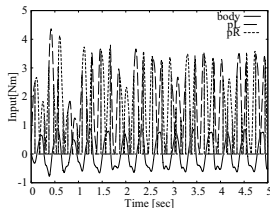


Fig. 13. Inputs on the simulation: τ_{tL}, τ_{tR} and τ_b are the input to the left thigh, the right thigh and the body.

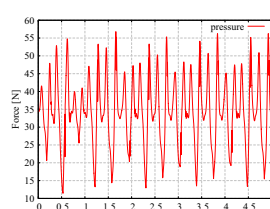


Fig. 14. The pressure F at CP of the Iwase-Åström model on the simulation.

From Fig. 11 and Fig. 12, it is confirmed that Iwase-Åström model is driven stably. From Fig. 13 and Fig. 14, it is confirmed that τ_{tL}, τ_{tR} and the pressure F are positive. Therefore the pedals are depressed by the cnemides in the driving simulation. From the Fig. 15, it is confirmed that MBP_w an opposite phase MBP_h. From the Fig. 16, it is confirmed behavior of the skilled rider which cross CP and MBP like the experiment.

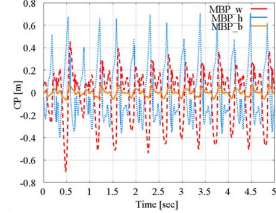


Fig. 15. MBP_w, MBP_h and MBP_b are elements of MBP in the Iwase-Åström model: MBP_w, MBP_h and MBP_b are MBP on the wheel torque, the hip torque and the body torque.

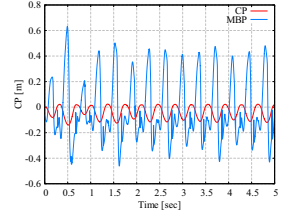


Fig. 16. The behavior of MBP and CP on the simulation.

VI. CONCLUSION

This paper tried to give an interpretation of the relationship between the MBP and the CP from the human motion viewpoint. A simple human-unicycle model, Iwase-Åström model, has been introduced for those analyses. The derivation of the modeling has been given by using the Projection Method, and the calculation of the MBP and the CP was also shown with the model. A simulation result show that MBP_w negate on MBP_h. By the result, the actual unicycle riding has some bearing on the behavior of the hip and the wheel. We will compare the model's behavior with experimental results circumstantially from not only the MBP and the CP but also other aspects.

REFERENCES

- [1] M. Iwase, M. Kinoshita, H. Ohsaki, Y. Sugimoto, K. Yoshida, H. Yoshida, and S. Hatakeyama, "Development of Dynamic Unicycle Simulator - From Human Adaptive Aspect-", *The 11th International Conference on Mechatronics Technology*, Ulsan, Korea, pp. 256-261, November 2007.
- [2] M. Kinoshita, K. Yoshida, Y. Sugimoto, H. Ohsaki, H. Yoshida, M. Iwase and S. Hatakeyama, "Support Control to Promote Skill of Riding a Unicycle", *IEEE International Conference on Systems, Man, and Cybernetics*, Suntec Singapore, Singapore, October 12-15, 2008.
- [3] Y. Naveh, P. Z. Bar-Yoseph and Y. Halevi, "Nonlinear Modeling and Control of a Unicycle", *Dynamics and Control*, Vol9, No.4, pp. 279-296, 1999.
- [4] S. V. Ulyanov, S. Watanabe, V. S. Ulyanov, K. Yamafuji, L. V. Litvinseva, and G. G. Rizzotto, "Soft Computing for the Intelligent Robust Control for a Robotic Unicycle with a New Physical Measure for Mechanical Controllability", *Soft Computing*, Vol. 2, pp. 73-88, 1998.
- [5] Z. Sheng and K. Yamafuji, "Realization of a Human Riding a Unicycle by a Robot", *IEEE International Conference on Robotics and Automation*, pp. 1319-1326, 1995.
- [6] Z. Sheng and K. Yamafuji, "Postural Stability of a Human Riding a Unicycle and Its Emulation by a Robot", *IEEE Trans. on Robotics and Automation*, Vol. 13, No. 5, pp.709-720, 1997.
- [7] Dmitry V. Zenkov and Anthony M. Bloch, "Stabilization of the Unicycle with Rider", *Proc. Of the 38th Conference on Decision and Control Phoenix*, Arizona, USA, 1999.
- [8] W. Blajer, "A Projection Method Approach to Constrained Dynamic Analysis", *J. Appl. Mech.* 59, pp.51-64, 1992.
- [9] W. Blajer and Arczewski K, "Unified Approach to the Modeling of Holonomic and Nonholonomic Mechanical Systems", *Mathematical Modeling of Systems*, Vol2, No.3, pp.157-174, 1996.
- [10] W. Blajer, "Projective Formulation of Lagrange's and Boltzmann-Hamel Equations for Multibody Systems.", *ZAMM 75 SI*, pp.S107 – S108, 1995.
- [11] W. Blajer, "A Geometrical Interpretation and Uniform Matrix Formulation of Multibody System Dynamics", *ZAMM 81*, Vol4, pp.247 – 259, 2001.
- [12] H.Ohsaki, M.Iwase and S.Hatakeyama, "A Consideration of Nonlinear System Modeling using the Projection Method", *SICE Annual Conference 2007*, Kagawa, Japan, September 17-20, pp. 1915 – 1920 2007.
- [13] H. Ohsaki, M. Iwase, T. Sadahiro and S. Hatakeyama, "Analysis and Modeling the Unicycle Considering the Unilateral Constraint between the Hip and the Saddle", *ECCOMAS Thematic Conference on Multibody Dynamics 2009*, Warsaw, Poland, June 29 - July 2, paper ID 295, 2009.